New Features of Bis(phosphinimine)-"carbene" Binding to Ru^{II}

Yegor Smurnyy, Christine Bibal, Maren Pink, and Kenneth G. Caulton*

Department of Chemistry, Indiana University, Bloomington, Indiana 47405, and M.V. Lomonosov Moscow State University, Moscow, Russia 119992

Received March 10, 2005

Analysis of the results of DFT(PBE) calculations on a variety of species containing a "RuC-$(PPh_2NPh)_2$" subunit led to the proposal that this should be considered as an example where an Ru/C single bond is present, which leaves a stereochemically active lone pair on the "carbene" carbon and thus a pyramidal, quasi-sp^3 hybridization for carbon. General applications of this idea are discussed, the possible protonation of this carbon lone pair is described, and a DFT(PBE) geometry optimization of the two species $(Cl)_nRuHC(PPh_2NPh)_2^{(1-n)+}$ with $n = 0, 1$ reveals a potential for oxidative addition of the P/N bond of this ligand to Ru, to generate an RuNPh moiety. The crystal structure of the triflate ($CF_3SO_3^-$) salt of the C-protonated species (Cymene)Ru[H*C$(PPh_2NPh]_2]^+$ shows that H* hydrogen bonds to triflate.

Introduction

We have been attracted to examine the highly varied coordination chemistry of bis-phosphinimine methanes, $H_2C(PR_2NR')_2$, and their related single and double deprotonation products. The singly deprotonated monoanion can bind η^2 through two N or η^3, through two N and the nucleophilic ring carbon. The latter form shows puzzling variability in the M/C distance, which we note but do not address here.[1−5] Instead, we focus here on the fully C-dehydrogenated form, **I**, which has the characteristics of a carbene, but one whose substituents are unusual in that both are electron-withdrawing groups.[6] Because **I** is not known in the free state, but

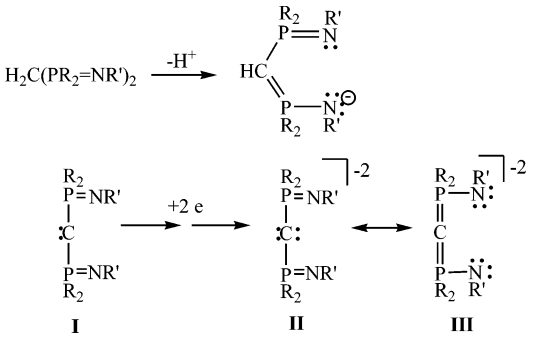

only coordinated to metals, its charge when coordinated to a metal can be ambiguous, and **II** and **III** show two resonance contributors to a doubly reduced form. Several examples where **I** is bidentate, through C and *one* N, to a metal (Pt) seem well-described as carbenes,[7] in these d^8 and planar species.

Results

Goals. Our approach has been to carry out DFT (PBE) geometry optimization of structures, including isomeric structures, concurrent with synthetic work with this ligand class attached to d^6, Ru(II) species.[8] This can identify which structures are *not* energy minima, as well as predict favored isomers from among several candidates. Given the unusual experimental structural and electronic features discussed above, the DFT results may also help to understand bond order and ligand atom hybridization; no self-consistent picture of these characteristics has emerged thus far for these unusual "carbenoid" ligands bearing two electron-withdrawing groups. In fact, the DFT calculations reported here permit a completely new interpretation of this metal carbenoid bond and also point the way to intriguing new synthetic goals.

(Arene)Ru[C$(PPh_2NPh)_2$]. Our particular goal was to contrast the available coordination chemistry of $C(PR_2NR')_2$ on early transition metals[9−12] with low d electron counts by the study of late metal complexes with higher d electron counts. Using all atoms of

(1) Hill, M. S.; Hitchcock, P. B. *J. Chem. Soc., Dalton Trans.* **2002**, 4694−4702.
(2) Evans, D. J.; Hill, M. S.; Hitchcock, P. B. *Dalton Trans.* **2003**, 570−574.
(3) Wei, P.; Stephan, D. W. *Organometallics* **2002**, *21*, 1308−1310.
(4) Gamer, M. T.; Dehnen, S.; Roesky, P. W. *Organometallics* **2001**, *20*, 4230−4236.
(5) Gamer, M. T.; Roesky, P. W. *J. Organomet. Chem.* **2002**, *647*, 123−127.
(6) Davies, H. M. L.; Beckwith, R. E. J. *Chem. Rev. (Washington, DC)* **2003**, *103*, 2861−2903.
(7) Jones, N. D.; Lin, G.; Gossage, R. A.; McDonald, R.; Cavell, R. G. *Organometallics* **2003**, *22*, 2832−2841.
(8) Bibal, C.; Pink, M.; Smurnyy, Y. D.; Tomaszewski, J.; Caulton, K. G. *J. Am. Chem. Soc.* **2004**, *126*, 2312−2313.
(9) Cavell, R. G.; Babu, R. P. K.; Kasani, A.; McDonald, R. *J. Am. Chem. Soc.* **1999**, *121*, 5805−5806.
(10) Kamalesh Babu, R. P.; Cavell, R. G.; McDonald, R. *Chem. Commun. (Cambridge)* **2000**, 481−482.
(11) Aparna, K.; Ferguson, M.; Cavell, R. G. *J. Am. Chem. Soc.* **2000**, *122*, 726−727.
(12) Watson, L. A.; Yandulov, D. V.; Caulton, K. G. *J. Am. Chem. Soc.* **2001**, *123*, 603−611.

10.1021/om050180r CCC: $30.25
Publication on Web 06/30/2005

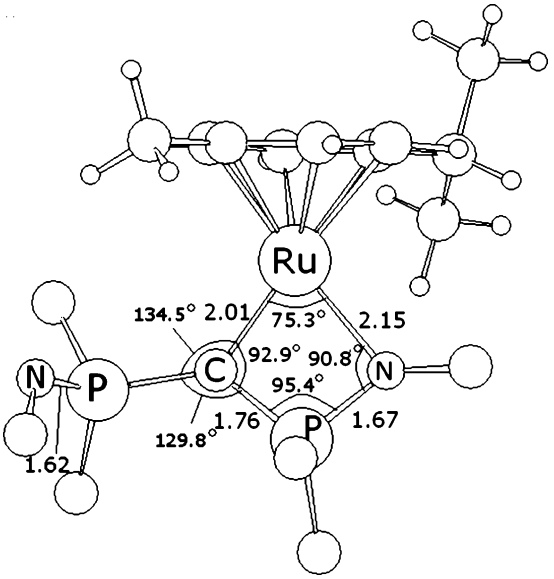

Figure 1. Calculated (DFT; distances in Å) structure of (Cymene)Ru η^2-[C(PPh$_2$NPh)$_2$]. Only the *ipso* carbons of phenyl groups are shown.

(Cymene)Ru[C(PPh$_2$NPh)$_2$] in a DFT(PBE) geometry optimization led to *two* stationary points, both minima. The first (**A** and Figure 1) has an η^2-chelate ligand, bound to Ru through a carbene carbon and one imine nitrogen. The second imine nitrogen lone pair is not

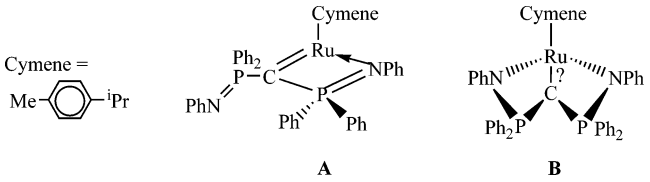

bound to Ru, consistent with avoidance of a 20 valence electron configuration at the metal. The CRuN plane is essentially perpendicular to the cymene ring plane. The Ru/C distance, 2.01 Å, is short enough to be considered a double bond (compare 2.22 Å for a Ru−C(sp^3) bond).[13] This Ru=C double bond localizes the ring P−C as a single bond and the P/N bond as double, in agreement with the bond lengths shown. The carbene carbon is nearly planar (angles sum to 357.2°).

The second minimum energy structure (**B** and Figure 2) is remarkable for having an η^3 "carbene" ligand. Equally remarkable is the fact that its energy is so similar to that of **A**: **B** is only 5.0 kcal/mol higher in free energy than **A**. We initially doubted this structure since it appeared to involve 20 valence electrons around Ru (assuming an Ru=C double bond) and thus reflects occupancy of a high-lying orbital. The Ru−C(cymene) distances gave no support for η^4-cymene binding. The alternative structure **C** would leave the carbene *carbon* truly unsaturated (the two carbene substituents, being electron withdrawing, cannot diminish this problem). It also requires energetically costly reduction of Ru, to Ru(0). However, if a σ bond exists between Ru(II) and carbon (**D**), then a Ru/C bond is formed *without* increasing the metal valence electron count above the 18

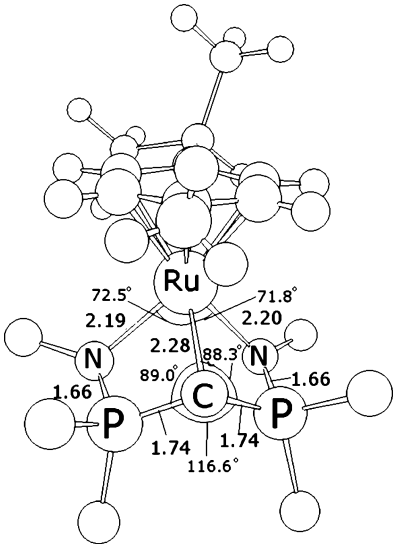

Figure 2. Calculated (DFT) structure of (Cymene)Ru η^3-[C(PPh$_2$NPh)$_2$]. Only the *ipso* carbons of phenyl groups are shown.

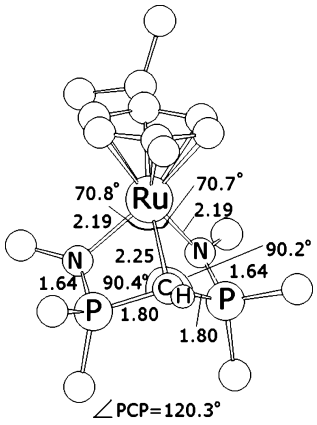

Figure 3. Calculated structure of (Cymene)Ru[HC(PPh$_2$NPh)$_2$]$^+$, showing only the *ipso* carbons of all phenyls.

present in **C** because a pair of electrons is localized on carbon. The Ru/C *single* bond implied by **D** is consistent

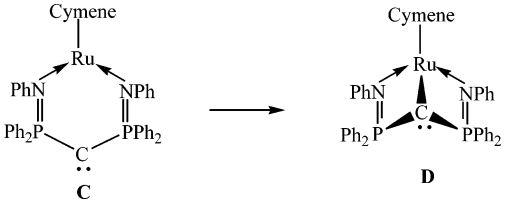

with the 2.28 Å distance found in this DFT structure (much longer than in **A)**. Also persuasive of this bonding picture is the highly pyramidal nature of the chelate ring carbon (the three angles sum to 293.9°), which confirms that there is a lone pair on this carbon, and thus the Ru/C bond is single, leaving a stereochemically active lone pair on carbon. The corresponding angle sum after protonation of this carbon (see next section and Figure 3) is 300.9°. The calculated[14,15] NBO charge on this carbon in **D** is remarkably negative (−1.17 e).

(13) Watanabe, M.; Murata, K.; Ikariya, T. *J. Am. Chem. Soc.* **2003**, *125*, 7508−7509.

(14) Reed, A. E.; Weinstock, R. B.; Weinhold, F. *J. Chem. Phys.* **1985**, *83*, 735−46.

(15) Reed, A. E.; Curtiss, L. A.; Weinhold, F. *Chem. Rev. (Washington, DC)* **1988**, *88*, 899−926.

Second-order perturbation theory analysis of the Fock matrix in the NBO basis shows the absence of any significant interaction of the carbon lone pair with any metal atomic orbital. This supports the interpretation of a carbon-localized lone pair. A comparison to phosphorus ylides, $R_3P^+-C^-H_2$, is thus appropriate.

While our work was under review, a publication appeared[16] on compound **E** and its deprotonation (dehydrochlorination) to give the carbene **F**, including a crystal structure determination of **F**. The main difference from our work here is the strongly electron-withdrawing substitutent on nitrogen in **E** and **F**. DFT calculations on **F** yield a natural population analysis charge on the carbene carbon of −1.19 e (which is much more negative than the −0.015 e calculated there for $RuCl_2(CH_2)(PMe_3)_2$), AND the authors analyze the HOMO as an Ru/C π bond (together with an Ru−C σ bond), which makes it analogous to our ground state structure (**A** and Figure 1). Our 5 kcal/mol higher energy isomer (i.e., η^3-ligand binding to Ru) in Figure 2 was not discussed in this recent work.

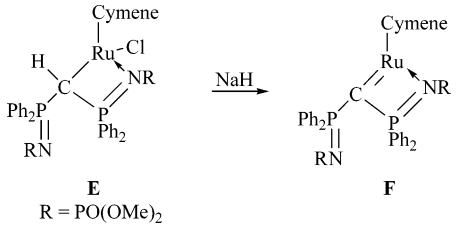

Protonation as Evidence of Bronsted Basicity of Isomer D. If the pyramidal geometry reliably indicates a lone pair on that carbon, it is reasonable to seek evidence of this by studying protonation at that site. Indeed, geometry optimization of (Cymene)Ru[HC(PPh$_2$NPh)$_2$]$^+$ shows a minimum energy structure (Figure 3) that resembles a three-legged piano stool. Despite protonation of the carbon, the Ru−C bond is retained. The optimum geometry does not relax to (Cymene)Ru[η^2-HC(PPh$_2$NPh)$_2$]$^+$, where the chelate binds through only two nitrogens. The Ru−C (single) bond length in this structure is 2.25 Å, which further supports the idea that only a Ru−C single bond exists in the deprotonated species (Cymene)Ru[η^3-C(PPh$_2$NPh)$_2$], which has Ru−C = 2.28 Å (Figure 2).

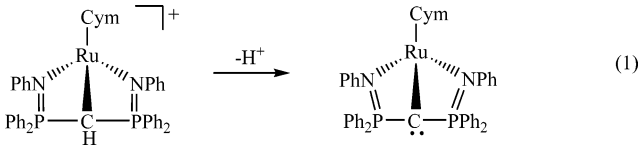

(1)

In effect, deprotonation (eq 1) of (Cymene)Ru[HC(PPh$_2$NPh)$_2$]$^+$ leaves the electrons of the C−H bond localized on that carbon. That carbon remains nonplanar.

A synthesis of this C-protonated cation has been accomplished (eq 2, Cym = 4-^{i}Pr-toluene), as its triflate ($CF_3SO_3^-$) salt. A single-crystal X-ray crystallographic determination of its structure (Figure 4 and Tables 1 and 2) shows good agreement with the DFT geometry-optimized structure of the isolated cation, confirming that the triflate counterion has no significant perturbing influence on the cation structure. The Ru−CH(PPh$_2$NPh)$_2$ distance (2.230(4) Å) compares well to that from the DFT calculation (2.25 Å). Of special interest is the fact that one of the triflate oxygens, O3, forms a hydrogen bond to the "methanide" hydrogen, with an H1A···O3 distance of 2.73 Å and an ∠C1−H1A···O3 of

$$(\mathrm{Cym})\mathrm{RuCl_2} \xrightarrow[(2)\ \mathrm{Me_3SiOTf}]{(1)\ \mathrm{LiHC(PPh_2NPh)_2}} (\mathrm{Cym})\mathrm{Ru[HC(PPh_2NPH)_2]^+} + \mathrm{F_3CSO_3^-} + \mathrm{Me_3SiCl} \quad (2)$$

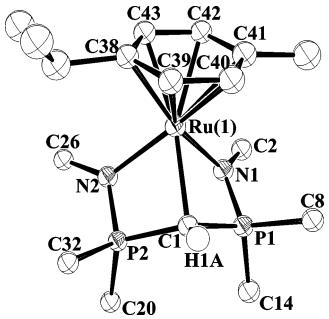

Figure 4. ORTEP drawing (50% probability) of the nonhydrogen atoms of (Cymene)Ru[HC(PPh$_2$NPh)$_2$]$^+$, showing selected atom labeling. The hydrogen on C1, which hydrogen bonds to triflate, is illustrated. Only the phenyl *ipso* carbons are shown.

Table 1. [RuCH(PPh$_2$NPh)$_2$(cym)](CF$_3$SO$_3$)·3THF

empirical formula	$C_{60}H_{69}F_3N_2O_6P_2RuS$
molecular weight	1166.24
instrument	SMART6000
cryst color, shape	orange plate
cryst size	0.21 × 0.18 × 0.10 mm^3
cryst syst	monoclinic
space group	*Cc*
cell dimens (130 K)	
a	28.993(3) Å
b	11.0780(11) Å
c	21.234(2) Å
α	90°
β	125.623(2)°
γ	90°
volume	5543.8(10) Å^3
Z (molecules/cell)	4
calcd density	1.397 Mg/mm^3
abs coeff	0.441 mm^{-1}
final residuals	
R1, observed data	0.0446[a]
wR2, all data	0.1095[b]

[a] $R1 = \Sigma(|F_o| - |F_c|)/\Sigma|F_o|$. [b] $wR2 = [\Sigma[w(F_o^2 - F_c^2)^2]/\Sigma[w(F_o^2)^2]]^{1/2}$.

Table 2. Selected Bond Lengths [Å] and Angles [deg] for the Cation (Cymene)Ru[HC(PPh$_2$NPh)$_2$]$^+$

Ru1−C1	2.230(4)	Ru1−N1	2.147(4)
P1−N1	1.618(4)	Ru1−N2	2.175(4)
P2−N2	1.608(4)	P1−C1	1.774(4)
Ru1−C38	2.131(19)	P2−C1	1.752(4)
Ru1−C43	2.15(2)	Ru1−C40	2.228(8)
Ru1−C39	2.172(10)	Ru1−C41	2.245(10)
Ru1−C42	2.205(19)	N1−Ru1−C1	71.45(14)
N1−Ru1−N2	84.92(15)	N1−P1−C1	97.7(2)
N2−Ru1−C1	70.14(14)	C2−N1−P1	128.4(3)
N2−P2−C1	97.7(2)	P1−N1−Ru1	97.85(17)
C2−N1−Ru1	132.2(3)	C32−N2−Ru1	131.2(3)
C32−N2−P2	131.2(3)	P2−C1−P1	119.4(2)
P2−N2−Ru1	95.12(17)	P1−C1−Ru1	90.40(18
P2−C1−Ru1	89.27(17)		

(16) Cadierno, V.; Diez, J.; Garcia-Alvarez, J.; Gimeno, J.; Calhorda, M. J.; Veiros, L. F. *Organometallics* **2004**, *23*, 2421−2433.

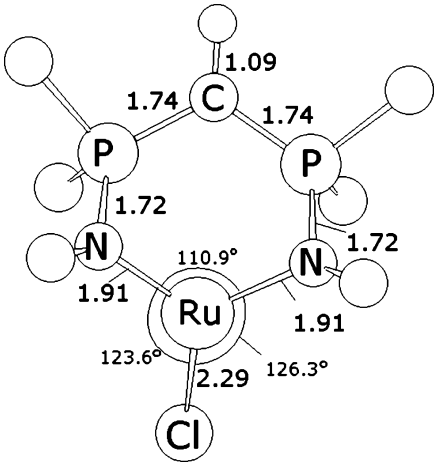

Figure 5. Calculated structure of ClRu[η^2-HC(PPh_2-$NPh)_2$], showing chair conformation of the six-membered ring.

157.6°. This is therefore experimental evidence that this is a positively polarized H on carbon and thus a candidate for the Bronsted acid/base reaction of eq 1.

In summary, deprotonation of the unique carbon produces a pair of electrons on the ligand. While the more stable product involves forming a Ru/C π bond while displacing one Ru/N bond (i.e., product **A**), only 5 kcal/mol worse is retention of these electrons as a lone pair on carbon, keeping both Ru/N bonds.

More Unsaturated Analogues. Exploration of a more unsaturated species, Ru[$HC(PPh_2NPh)_2$]Cl, has led to new insights about how this bis(phosphinimine) ligand might react toward highly unsaturated metals. In the absence of the six electrons donated to Ru by the cymene ligand, one stationary point on the potential energy surface is an η^2-ligand structure (Figure 5) where the metal is three-coordinate and planar, the six-membered ring is nonplanar and in a chair conformation, and the structure has idealized mirror symmetry (**G**). It is important to note that the ring conformation leaves the nitrogens coplanar with its attached Ru, C (*ipso*), and P and that this tends to reduce vicinal Ph(N)/Ph(P) repulsions. In response to the unsaturation at Ru, the Ru−N distances are very short and the P−N distances are long (cf. Figure 3), consistent with participation by resonance structure **H**. This charge-

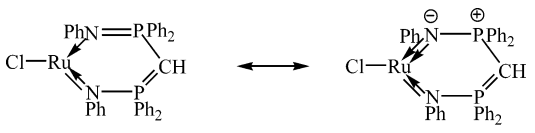

G **H**

separated form, with a P^+-N^- single bond, has been emphasized recently.[17] What is remarkable is that there is another energy minimum, and this structure is *more stable* by 13.0 kcal/mol ($\Delta G°$). In this (Figure 6), one P/N bond has been cleaved. The Ru coordination number is now four, because the ligand carbon now binds to Ru, forming a (monoanionic)bidentate ligand via a four-membered ring. The P/N bond cleavage occurs by two-electron oxidation of Ru (i.e., the metal oxidation state in Figure 5 is II, while in Figure 6 it is IV), and the

(17) Kocher, N.; Leusser, D.; Murso, A.; Stalke, D. *Chemistry−A Eur. J.* **2004**, *10*, 3622−3631.

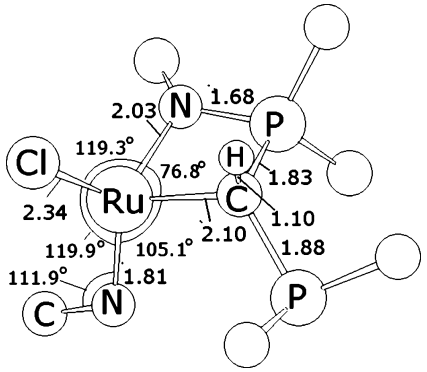

Figure 6. Calculated structure of ClRu(NPh)[η^2-HC(PPh_2-NPh)PPh_2].

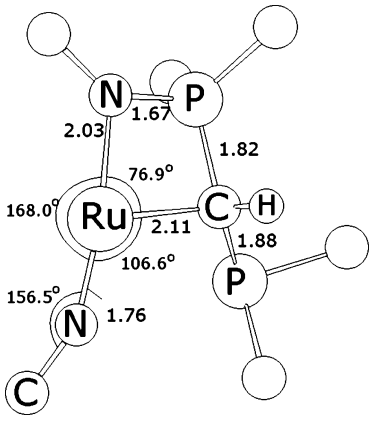

Figure 7. Calculated structure of Ru(NPh)[η^2-HC(PPh_2-NPh)PPh_2]$^+$.

thermodynamic preference for this P/N cleaved form may be attributed to the increased valence electron count coming from the NPh ligand. The latter is significantly bent ($\angle Ru-N-C_{(ipso)} = 111.9°$), suggesting Ru=N double bond character (Ru/N distance = 1.81 Å). We have done a parallel calculation on the analogue where all the phosphorus substituents have been changed from phenyl to methyl (to alter electrophilicity of the PR_2 groups), and the thermodynamic preference for the P/N cleavage isomer is essentially unchanged in magnitude (free energy 14.5 kcal/mol more stable than ClRu[η^2-$HC(PMe_2NPh)_2$]), and the structure is also little changed: Ru−N = 1.81 Å and $\angle Ru-N-C_{ipso} = 108.4°$. Thus, for this species, the ligand oxidation of Ru is not critically dependent on an electron-withdrawing phenyl on P.

Note that it is the carbon, not the newly reduced trivalent phosphorus that donates to the metal in RuCl(NPh)[$HC(PPh_2)PPh_2NPh$]. Although the imide ligand is not linear (i.e., not donating its maximum) in ClRu(NPh)[$HC(PPh_2)(PPh_2NPh)$], the optimized geometry for the product *without* a chloride ligand, i.e., the cation Ru(NPh)[$HC(PPh_2NPh)$]$^+$, shows that the imide ligand responds (Figure 7) to enhanced electron deficiency at Ru by increasing the $\angle Ru-N-C_{ipso}$ to 156.5° and a shortened Ru/N distance of 1.76 Å. In this cation, Ru is moving toward coplanarity with its three ligands: the sum of angles at Ru is 351.5°. The HC−PPh_2 distance to trivalent P, 1.88 Å, is a useful comparison standard of a single-bond distance. Other P−C distances reported here are invariably shorter, due to delocalization of the "carbene" lone pair toward P^V.

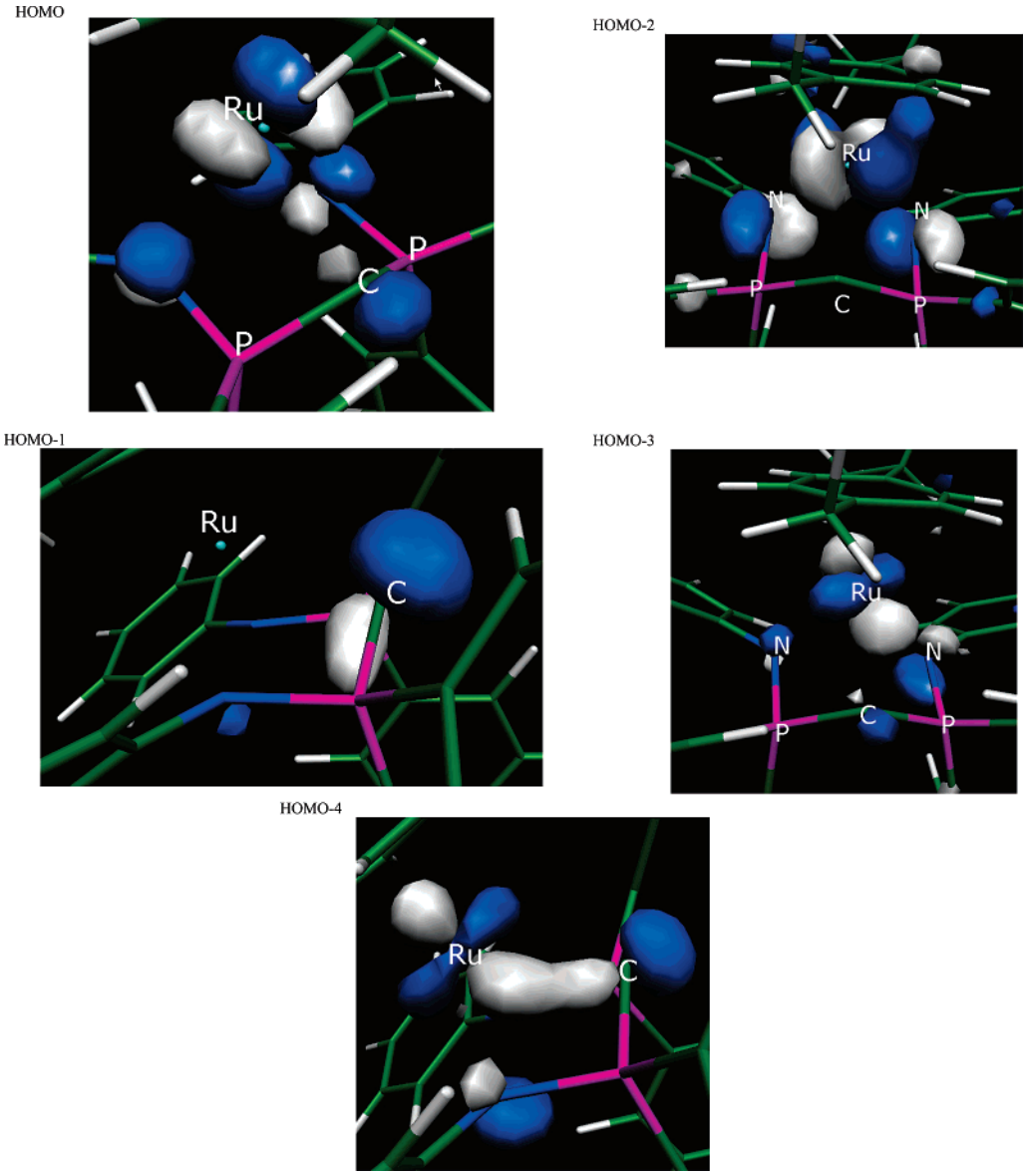

Figure 8. Representation of AO composition of the highest five filled orbitals of (Cym)Ru[η^3-C(PPh$_2$NPh)$_2$] showing the ring carbon "lone pair" (HOMO-1) and three doubly occupied, mainly d orbitals.

Discussion

Oxidation State Ambiguity. Reports of the (R′N=PR$_2$)$_2$C: carbene on four-coordinate platinum, but in a planar metal coordination geometry, have twice[7,18] been recognized as somewhat paradoxical (Pt^{II} vs Pt^0, the latter most often tetrahedral). At the heart of this paradox is the question of "correct" oxidation state for *this* carbene. To better understand this and the related question of M/C bond order, we next analyze the orbitals and the electron density calculated for the isomer **D** (Figure 2) of (Cymene)Ru[η^3-C(PPh$_2$NPh)$_2$].

Orbital Character of Ru/C Bonding. Examination of the orbitals of this less stable isomer **D** of (Cymene)-Ru[C(PPh$_2$NPh)$_2$], with an η^3-ligand, shows the transannular Ru/C orbital interaction. Figure 8 shows that the HOMO, HOMO-2, and HOMO-3 are mainly localized on the metal and give a d^6 electron count characteristic of Ru(II). HOMO-1 is the carbon lone pair, directed outward (i.e., away from Ru) and in the P−C−P plane. HOMO-4 is the Ru/C (single) bond and involves primarily that carbon orbital that is perpendicular to the P−C−P plane.

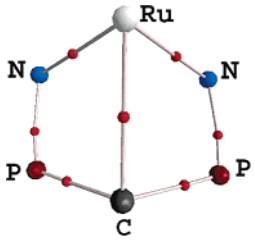

Figure 9. Drawing of the nuclear positions (labeled), bond paths (pink), and (3; −1) bond critical points (red), showing bonds, for (Cym)Ru[η^3-C(PPh$_2$NPh$_2$].

A map of the bond critical points[19] (Figure 9) is consistent with these conclusions from Lewis structures, and also from the orbital contours, in showing Ru−N,

(18) Lin, G.; Jones, N. D.; Gossage, R. A.; McDonald, R.; Cavell, R. G. *Angew. Chem., Int. Ed.* **2003**, *42*, 4054−4057.

(19) Bader, R. F. W. *Atoms in Molecules: A Quantum Theory*; Oxford University Press: Oxford, 1990.

Scheme 1

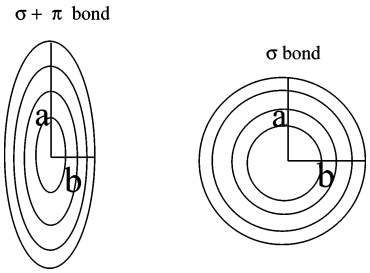

Table 3. Bond Ellipticities in (Cymene)Ru[η^3-C(PPh_2NPh_2]

	Ru−N	N−P	P−C	Ru−C
ellipticity	0.229	0.123	0.072	0.043

N−P, and P−C bonds (bond critical points in red). The bond critical point between Ru and C shows that the Ru/C internuclear vector thus qualifies as a "bond" in the same way as do the Ru−N, NP, and P−C vectors. The character (single or double) of this Ru/C interaction is revealed by the ellipticity parameters.

Ellipiticity[19] is a ratio of two negative eigenvalues of Hessian of the electron density. The Hessian matrix is calculated at the bond critical point (i.e., (3:−1) critical point). It can be rationalized as a measure of how cylindrically symmetric a bond is at the critical points in Figure 9. In particular, it can be used to distinguish a σ single bond from a $\sigma + \pi$ double bond. While a cylindrically symmetric σ bond has ellipiticity near zero, the elongated cross section of a π bond (Scheme 1) has nonzero ellipticity (which is defined as $a/b - 1$, calculated at the bond critical points in Figure 9). The ellipticity values shown in Table 3 confirm that the P/N bond contains considerable π character, with some P/C π character. The Ru/C bond contains the least π-character, consistent with it being a single (and σ) bond. The π character indicated for the Ru/N bond is consistent with participation by resonance structure **J**, which delocalizes negative formal charge away from carbon, and also accounts for the nonzero ellipticity value for the P/C bond.

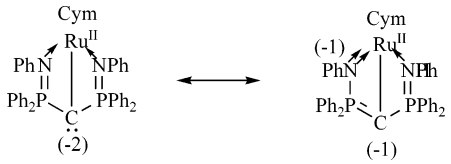

I **J**

Perspective. It is valuable to document the extent to which DFT-based geometry searches can actually reveal unanticipated structures: those that involve more than mere angular distortions and bond length *changes* but represent instead formation or breaking of bonds. For example, in studying the *transition state* for C−H bond cleavage by $RhCl(PH_3)_2$, a σ bond complex of intact methane $RhCl(PH_3)_2(\eta^2\text{-}HCH_3)$ was found[20] as an energy *minimum* (not merely a transition state). The same discovery was true of $(C_5H_5)Rh(CO)$ with methane.[21] The fact that, in the present work, the product of cleavage of a P=N bond was the energy minimum optimized starting from the intact $HC(Ph_2P{=}NPh)_2$ group on a (highly) unsaturated Ru(II) center gives cause for optimism that geometry searches using DFT can truly make discoveries beyond the intuition of the investigator. This is a very powerful accomplishment of the method; theory leads rather than follows. Cleavage of P=N bonds in bis-phosphimine methanide ligands therefore might be observed experimentally. Moreover, the ability of the geometry search algorithm to find a path that actually cleaves a P/N bond suggests that any barrier between the starting and final geometries, if it exists, must be less than about 5−10 kcal/mol, and thus the bond cleavage mechanism on the singlet energy surface will in actuality be kinetically facile at modest temperature.

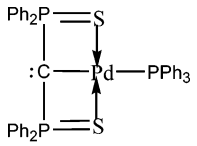

K

Finally, others[22] have recently reported an analogous bonding situation **K** in a closely related ligand. Their conclusion, like ours here, is that a Pd−C single bond exists, together with a carbon-centered lone pair. The noteworthy geometric feature is a pyramidal carbon.

Experimental Section

Computational Details. Theoretical calculations in this work have been performed using density functional theory,[23] with the PBE[24] functional, implemented in an original program package "Priroda" authored by Dr. D. N. Laikov.[25,26] Relativistic Stevens−Basch−Krauss (SBK) effective core potentials (ECP)[27−29] optimized for DFT calculations have been used. A Gaussian-type TZ2p basis set was used: Ru [5,1,1,1,1/5,1,1,1,1/5,1,1,1], C,N,P,Cl [3,1,1/3,1,1/1,1], H [3,1,1/1]. Full geometry optimizations have been performed without symmetry constraint. For all species under investigation, frequency analysis has been carried out, and zero-point vibration energy corrections have been made. All energies given are Gibbs standard free energies (298 K). During the frequency analysis, second derivatives were evaluated analytically. All geometries have been checked for the absence of imaginary frequencies. Topological analysis of the density function was performed with the XAIM package.[30] The wave function was obtained using the Gaussian 98 package;[31] a single-point calculation (DFT, PBE functional, custom TZ2p basis set) was performed using the previously optimized geometry, and no ECP was introduced.

(20) Koga, N.; Morokuma, K. *J. Am. Chem. Soc.* **1993**, *115*, 6883−92.
(21) Musaev, D. G.; Morokuma, K. *J. Am. Chem. Soc.* **1995**, *117*, 799−805.
(22) Cantat, T.; Mezailles, N.; Ricard, L.; Jean, Y.; Le Floch, P. *Angew. Chem., Int. Ed.* **2004**, *43*, 6382−6385.
(23) Parr, R. G.; Yang, W. *Density-functional Theory of Atoms and Molecules*; 1989.
(24) Perdew, J. P.; Burke, K.; Ernzerhof, M. *Phys. Rev. Lett.* **1996**, *77*, 3865−3868.
(25) Laikov, D. N. *Chem. Phys. Lett.* **1997**, *281*, 151−156.
(26) Ustynyuk, Y. A.; Ustynyuk, L. Y.; Laikov, D. N.; Lunin, V. V. *J. Organomet. Chem.* **2000**, *597*, 182−189.
(27) Cundari, T. R.; Stevens, W. J. *J. Chem. Phys.* **1993**, *98*, 5555−65.
(28) Stevens, W. J.; Basch, H.; Krauss, M. *J. Chem. Phys.* **1984**, *81*, 6026.
(29) Stevens, W. J.; Krauss, M.; Basch, H.; Jasien, P. G. *Can. J. Chem.* **1992**, *70*, 612−630.
(30) Ortiz, J. C.; Bo, C. Universitat Rovira i Virgili, Tarragona, Spain.

General Experimental. All synthetic work described was carried out using standard Schlenk techniques or a glovebox filled with argon. Solvents were dried and degassed before use. $H_2C(PPh_2NPh)_2$ and $(RuCl_2Cym)_2$ were synthesized according to the literature procedures.[32,33]

Preparation of CymRuCH(PPh$_2$NPh)$_2^+$Cl$^-$. Methyllithium

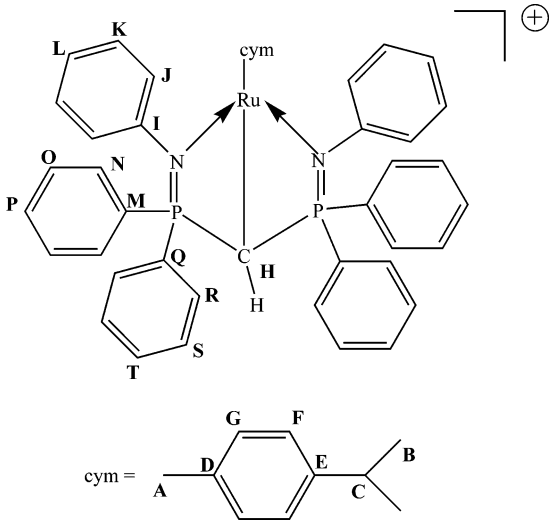

(0.41 mmol, 0.26 mL) was added dropwise to a stirred solution of $CH_2(PPh_2NPh)_2$ (0.2 g, 0.35 mmol) in THF at room temperature. After 20 min, the lithium salt (0.35 mmol) was slowly added to the dimer $(RuCl_2Cym)_2$ (0.1 g, 0.17 mmol) in THF at room temperature, and the reaction mixture was stirred overnight. Solvent was removed under vacuum, and the residue was extracted with toluene. A red powder was isolated from the toluene-soluble fraction after cooling the solution at −25 °C for 1 day (0.22 g, 78%). Mp: 218 °C (dec). ^{1}H NMR [499.8 MHz, CD_2Cl_2] (δ, ppm): 0.74 (d, $C(H_B)_3$, $^3J_{H/H}$ = 7 Hz, 6H); 1.53 (s, $C(H_A)_3$, 3H); 1.96 (sept, CH_C, $^3J_{H/H}$ = 7 Hz, 1H); 2.79 (s, PCH_HP, 1H); 5.25 (d, H_G, $^3J_{H/H}$ = 6 Hz, 2H); 5.32 (d, H_F, $^3J_{H/H}$ = 6 Hz, 2H); 6.82 (ddd, H_S, $^3J_{H/H}$ = 7.8 Hz, $^3J_{H/H}$ = 8.0 Hz, $^4J_{P/H}$ = 2.9 Hz, 4H); 6.94 (tt, H_L, $^3J_{H/H}$ = 7.3 Hz, $^4J_{H/H}$ = 1.4 Hz, 2H); 7.01 (ddd, H_R, $^3J_{H/H}$ = 8.0 Hz, $^4J_{H/H}$ = 1.3 Hz, $^3J_{P/H}$ = 12.8 Hz, 4H); 7.10 (m, H_T, $^3J_{H/H}$ = 7.8 Hz, $^4J_{H/H}$ = 1.3 Hz, $^5J_{P/H}$ = 1.5 Hz, 2H); 7.21 (dd, H_K, $^3J_{H/H}$ = 7.3 Hz, $^3J_{H/H}$ = 8.0 Hz, 4H); 7.25 (dd, H*J*, $^3J_{H/H}$ = 8.0 Hz, $^4J_{H/H}$ = 1.4 Hz, 4H); 7.71 (m, H_P, $^3J_{H/H}$ = 7.0 Hz, $^4J_{H/H}$ = 1.0 Hz, $^5J_{P/H}$ = 1.6 Hz, 2H); 7.74 (ddd, H_O, $^3J_{H/H}$ = 7.0 Hz, $^3J_{H/H}$ = 8.4 Hz, $^4J_{P/H}$ = 2.6 Hz, 4H); 8.25 (ddd, H_N, $^3J_{H/H}$ = 8.4 Hz, $^4J_{H/H}$ = 1.0 Hz, $^3J_{P/H}$ = 12.1 Hz, 4H). ^{31}P NMR [162.0 MHz, CD_2Cl_2] (δ, ppm): 34.23 (s). ^{13}C NMR [125.7 MHz, CD_2Cl_2] (δ, ppm): −21.35 (t, C_HH, $^1J_{P/C}$ = 86.1 Hz); 18.17 (s, C_AH_3); 22.41 (s, C_BH_3); 30.30 (s, C_CH); 81.12 (s, C_FH); 83.82 (s, C_GH); 96.10 (s, C_D); 106.19 (s, C_E); 121.18 (s, C_LH); 124.38 (d, C_JH, $^3J_{P/C}$ = 13.0 Hz); 128.58 (d, C_SH, $^3J_{P/C}$ = 12.2 Hz); 129.22 (s, C_K); 129.83 (d, C_OH, $^3J_{P/C}$ = 12.2 Hz); 130.94 (d, C_Q, $^1J_{P/C}$ = 71.3 Hz); 131.60 (d, C_RH, $^3J_{P/C}$ = 11.5 Hz); 131.71 (dd, C_M, $^1J_{P/C}$ = 84.7 Hz, $^3J_{P/C}$ = 8.7 Hz); 132.28 (s, C_TH); 132.41 (d, C_NH, $^3J_{P/C}$ = 10.7 Hz); 133.48 (s, C_P); 148.82 (s, C_I). FAB MS (m, intensity): 801 (M, 28), 667 (M − cym, 100), 589 (M − cym − H$^+$ − Ph, 26).

Preparation of CymRuCH(PPh$_2$NPh)$_2^+$OTf$^-$. Me_3SiOTf

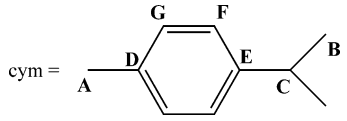

(10 μL, 0.05 mmol) was added with a microsyringe to a solution of $CymRuCH(PPh_2NPh)_2^+Cl^-$ (25 mg, 0.03 mmol) in benzene. Single crystals were obtained from a solution of $CymRuCH(PPh_2NPh)_2^+OTf^-$ in THF cooled at −25 °C for several days. ^{1}H NMR [400.1 MHz, C_6D_6] (δ, ppm): 0.55 (d, $C(H_B)_3$, $^3J_{H/H}$ = 7.2 Hz, 6H); 1.24 (s, $C(H_A)_3$, 3H); 1.98 (sept, CH_C, $^3J_{H/H}$ = 7.2 Hz, 1H); 3.12 (s, PCHP, 1H); 5.06 (d, H_G, $^3J_{H/H}$ = 5.6 Hz, 2H); 5.25 (d, H_F, $^3J_{H/H}$ = 5.6 Hz, 2H); 6.28−8.41 (m, aryl-H, 30H). ^{31}P NMR [162.0 MHz, C_6D_6] (δ, ppm): 35.53 (s). ^{13}C NMR [100.6 MHz, C_6D_6] (δ, ppm): −22.71 (t, PCHP, $^1J_{P/C}$ = 86.9 Hz); 17.89 (s, C_AH_3); 22.22 (s, C_BH_3); 30.07 (s, C_CH); 81.25 (s, C_FH); 84.05 (s, C_GH); 95.49 (s, C_D); 105.54 (s, C_E); 120.77−149.62 (aryl-C).

X-ray Structure Determination of {(Cymene)Ru[HC(PPh$_2$NPh)$_2$]}O$_3$SCF$_3$·3THF. A red crystal (approximate dimensions 0.21 × 0.18 × 0.10 mm^3) was placed onto the tip of a 0.1 mm diameter glass capillary and mounted on a SMART6000 (Bruker) at 130(2) K. The data collection (Table 1) was carried out using Mo Kα radiation (graphite monochromator) with a frame time of 20 s and a detector distance of 5.0 cm. A randomly oriented region of reciprocal space was surveyed to the extent of a sphere. Four major sections of frames were collected with 0.30° steps in ω at different ϕ settings and a detector position of −43° in 2θ. Data to a resolution of 0.80 Å were considered in the reduction. Final cell constants were calculated from the *xyz* centroids of 7374 strong reflections from the actual data collection after integration. The intensity data were corrected for absorption. The ruthenium complex crystallizes with one triflate anion and three molecules of THF. *p*-Cymene is disordered over two positions (50:50), rotating almost 180°. The distance of Ru to the center of the phenyl ring (C38, ...C43) is 1.70 Å and to the center of the phenyl ring (C38d, ...C43d) 1.72 Å. Two THF molecules are disordered over two positions and were refined with a set of restraints and constraints.

Acknowledgment. This work was supported by the National Science Foundation. We also thank Prof. Y. A. Ustynyuk (Moscow State University) for his support of this project, and Dr. D. Laikov for use of his software. Computations were done at the Russian Academy of Sciences joint supercomputer center.

Supporting Information Available: Full crystallographic details as a cif file and also Cartesian coordinates of all structures illustrated. This material is available free of charge via the Internet at http://pubs.acs.org.

OM050180R

(31) Frisch, M. J.; Trucks, G. W.; Schlegel, H. B.; Scuseria, G. E.; Robb, M. A.; Cheeseman, J. R.; Zakrzewski, V. G.; Montgomery, J. A.; Stratmann, R. E.; Burant, J. C.; Dapprich, S.; Milliam, J. M.; Daniels, A. D.; Kudin, K. N.; Strain, M. C.; Farkas, O.; Tomasi, J.; Barone, V.; Cossi, M.; Cammi, R.; Mennucci, B.; Pomelli, C.; Adamo, C.; Clifford, S.; Ochterski, J.; Petersson, G. A.; Ayala, P. Y.; Cui, Q.; Morokuma, K.; Malick, D. K.; Rabuck, A. D.; Raghavachari, K.; Foresman, J. B.; Cioslowski, J.; Ortiz, J. V.; Stefanov, B. V.; Liu, G.; Liashenko, A.; Piskorz, P.; Komaromi, I.; Gomperts, R.; Martin, R. L.; Fox, D. J.; Keith, T.; Al-Laham, M. A.; Peng, C. Y.; Nanayakkara, A.; Gonzalez, C.; Challacombe, M.; Gill, P. M. W.; Johnson, B. G.; Chen, W.; Wong, M. W.; Andres, J. L.; Head-Gordon, M.; Replogle, E. S.; Pople, J. A. *Gaussian 98* (Revision; A.97); Gaussian, Inc.: Pittsburgh, PA, 1998.

(32) Al-Benna, S.; Sarsfield, M. J.; Thornton-Pett, M.; Ormsby, D. L.; Maddox, P. J.; Bres, P.; Bochmann, M. *Dalton* **2000**, 4247−4257.

(33) Bennett, M. A.; Huang, T. N.; Matheson, T. W.; Smith, A. K. *Inorg. Synth.* **1982**, *21*, 74−8.